Lemos, Janyelle de Oliveira; Freire, Fernando José; Souza, Valdomiro Severino de; Oliveira, Emídio Cantídio Almeida de; Lucena, Pedro Gabriel Correia de; Silva, Suellen Roberta Vasconcelos da; Freire, Maria Betânia Galvão dos Santos; Lima, Danubia Ramos Moreira de

Phosphorus fractions in soils with distinct mineralogy and their relationship with phosphate buffer capacity indicators in Brazil

SOILS

Phosphorus fractions in soils with distinct mineralogy and their relationship with phosphate buffer capacity indicators in Brazil

Janyelle de Oliveira Lemos[1], Fernando José Freire[1]*, Valdomiro Severino de Souza Júnior[1], Emídio Cantídio Almeida de Oliveira[1], Pedro Gabriel Correia de Lucena[2], Suellen Roberta Vasconcelos da Silva[1], Maria Betânia Galvão dos Santos Freire[1] and Danubia Ramos Moreira de Lima[1]

[1]Departamento de Agronomia, Universidade Federal Rural de Pernambuco, Av. Dom Manuel de Medeiros, s/n, 52171-900, Recife, Pernambuco, Brazil. [2]Departamento de Química, Universidade Federal de Pernambuco, Recife, Pernambuco, Brazil. *Author for correspondence. E-mail: fernando.freire@ufrpe.br

ABSTRACT. Phosphorus (P) is one of the most important elements used in fertilizing soils in tropical regions due to the low efficiency of phosphate fertilization. This work aimed to fractionate inorganic P (Pi) in tropical soils of different mineralogical compositions and to relate these fractions with their respective phosphate buffer capacity (PBC) indicators. The soils were characterized physically, chemically and mineralogically. Additionally, we evaluated the P concentration that remained in solution of soil after equilibrium was met; this was termed P remaining (P-rem). In general, the Pi fractions of soils did not correlate with the PBC indicators. The P-H_2O fraction showed a negative correlation with the P-Al fraction. Ferric minerals did not influence P fixation. P-rem showed a strong correlation with the maximum P adsorption capacity, adsorption energy, and the amorphous and crystalline forms of Fe. The minerals of aluminum contributed the most to P fixation. P-rem was the best estimator of PBC. The soils with high, moderate and low rates of P fixation showed high amounts of the fractions P-Al, P-Ca, and P-Fe, respectively. The results showed that P fixation was influenced by the fractions of P in the soil, suggesting that the efficiency of phosphate fertilizers in tropical soils depends on the mineralogy of the clay fraction within those soils.

Keywords: P fixation; sequential fractionation of P; vertisols; cambisols; ferralsols.

Introduction

The use of P in fertilization in tropical soils is high, mainly because tropical soils result in low P fertilization efficiency. The high capacity of P fixation in these regions is related to the high interaction dynamics between P and other mineralogical constituents within the soil (Fink et al., 2016a; Fink, Inda Junior, Tiecher, & Barrón, 2016b), resulting in the reduced availability of P.

Fractionation methods have been used to understand different P fractions within soil. There are several methods for quantifying P fractions within soil. The sequential fractionation method of soil is based on the different solubilities of P forms (Abdala, Silva, Vergütz, & Sparks, 2015) and is the most commonly used (Nishigaki et al., 2018). This method uses extractors capable of selectively extracting several fractions of inorganic P (Pi), such as soluble P (P-H_2O), extracted by NH_4Cl; P associated with Al (P-Al), extracted by NH_4F; P associated with Fe (P-Fe), extracted by NaOH; and P associated with Ca (P-Ca), extracted by H_2SO_4. These studies are of great importance in evaluating the dynamics of P as a function of soil mineralogy (Souza Júnior, Oliveira, Santos, Freire, & Arruda, 2012).

The P fixation in oxidic soils is greater, with goethite and gibbsite being the main mineralogical constituents responsible for this phenomenon (Fink et al., 2016a; Fink et al., 2016b). Silicate clays with a 1:1 ratio, such as kaolinite, have less capacity to adsorb P, which can be attributed to their smaller specific surface area (Christophe, Bourg, Steefel, & Bergaya, 2015). The point of zero charge (PZC) of kaolinite is another factor responsible for the lower contribution of this clay mineral to P adsorption when compared with the oxides of Fe and Al. The PZC of kaolinite varies between 2.0 and 3.1 according to Khawmee, Suddhiprakarn, Kheoruenromne, and Singh (2013). Thus, the predominant surface charge of this mineral in cultivated soils (pH > 4.0) is electronegative, decreasing the adsorption between the phosphate and the adsorbent surface.

The influence of mineralogy on P dynamics has been the subject of many studies (Eriksson, Hesterberg, Klysubun, & Gutafsson, 2016) that aim to identify the causes of P unavailability. Phosphate fertilization recommendations can be influenced by the mineralogy of the soil. For example, the amount and source of P fertilizer, as well as the application method, can vary depending on the mineralogy of the soil, allowing farmers to more adequately manage phosphate fertilization in tropical regions.

Our hypothesis is that soils with a predominance of kaolinite within the clay fraction adsorb less P because of their higher association with Ca and lower association with Fe and Al. Our expectation is that in kaolinitic soils rich in Ca, the relationship of the fixation of P is with the P-Ca fraction. Thus, this work aimed to fractionate Pi in tropical soils of different mineralogical compositions and to relate the fractions of P with the corresponding phosphate buffer capacity (PBC) indicators of these soils.

Material and methods

Study area and soil sampling

The study was carried out with samples of seven soils from areas close to large productive arrangements in Brazil located in the states of Bahia, Paraíba, Rio Grande do Norte, Goiás, Piauí, and Pernambuco (Figure 1). Soil samples were collected in reserve areas for environmental protection in secondary forests within agricultural farms.
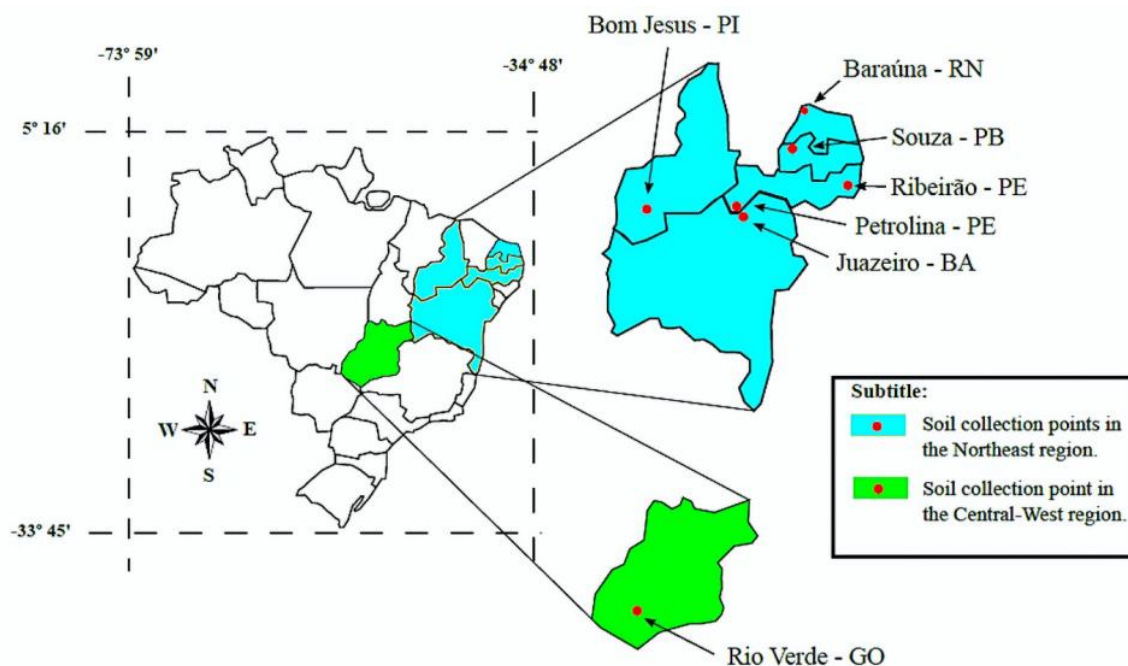

Figure 1. Study areas location map.

The municipalities where soil samples were collected have the following climatic characteristics: Juazeiro, Bahia (BA) State, BSh climate, average annual temperature of 24.8°C, average annual rainfall of 422 mm; Souza, Paraíba (PB) State, Aw climate, average annual temperature of 26.7°C, average annual rainfall of 872 mm; Baraúna, Rio Grande do Norte (RN) State, Aw climate, average annual temperature of 27.3°C, average annual rainfall of 859 mm; Rio Verde, Goiás (GO) State, Aw climate, annual average temperature of 23.3°C, average annual rainfall of 1,663 mm; Bom Jesus, Piauí (PI) State, Aw climate, average annual temperature of 28°C, average annual rainfall of 1,000 mm; Ribeirão, Pernambuco (PE) State, Am climate, average annual temperature of 24°C, average annual rainfall of 1,866 mm; Petrolina, Pernambuco (PE) State, Brazil, BSh climate, average annual temperature of 24.8°C, average annual rainfall of 435 mm. The climatic classification was carried out according to the Köppen classification (Alvares, Stape, Sentelhas, Gonçalves, & Sparovek, 2013) and climatic characteristics according to INMET (2020).

The soils sampled were Haplic Vertisol (Calcaric), (VRha$_1$); Haplic Sodic Vertisol, (VRha$_2$); Calcaric Leptic Cambisol, (CMle); Geric Acric Ferralsol, (FRac); Geric Ferralsol (Dystric), (FRgr$_1$); Geric Ferralsol (Dystric), (FRgr$_2$) and Ferralsol (Eutric, Loamic), (FReu), classified according to IUSS Working Group WRB (2014). The

soils were chosen according to the mineralogical composition of the clay fraction (kaolinite, smectite, hematite, goethite, gibbsite and rich in Fe and Al oxide) (Table 1).

Table 1. Identification of studied soils, with their respective parent material and collection location.

Soils	Identification	Parent material	Collection location
Haplic Vertisol (Calcaric)	VRha$_1$	Limestone of the Caatinga Formation	Juazeiro – BA
Haplic Sodic Vertisol	VRha$_2$	Cretaceous clay	Souza – PB
Calcaric Leptic Cambisol	CMle	Limestone	Baraúna – RN
Geric Acric Ferralsol	FRac	Basalt of the Serra Geral Formation	Rio Verde – GO
Geric Ferralsol (Dystric)	FRgr$_1$	Pre-weathered clay-sand sediment	Bom Jesus – PI
Geric Ferralsol (Dystric)	FRgr$_2$	Granite/gneiss suites	Ribeirão – PE
Ferralsol (Eutric, Loamic)	FReu	Sedimentary coating (Pediment)	Petrolina – PE

The number of samples needed to accurately represent the soil properties (sample adequacy) was calculated according to Snedecor and Cochran (1967). Sampling was performed after delineating a 100 x 100 m square within each study area. Twenty-five samples were collected in this square, spaced 25 m x 25 m at depths of 0-20 cm and 20-40 cm, totaling 50 samples per area (350 samples in total). Samples were collected with a screw auger that deformed the structure of the soil sample.

Physical and chemical analysis

Physically, only the clay fraction content was determined by the pipette method, with the modifications proposed by Ruiz (2005). Chemically, the soils were characterized for pH (H_2O), pH (KCl), Ca^{2+}, Mg^{2+}, K^+, Al^{3+}, Na^+, (H+Al), P, total organic carbon (TOC), and total nitrogen (TN). Ca^{2+}, Mg^{2+} and Al^{3+} were extracted by 1.0 mol L^{-1} KCl, while P, K^+, and Na^+ were extracted by Mehlich-1. Potential acidity (H+Al) was extracted with 0.5 mol L^{-1} calcium acetate and measured by titration. Ca^{2+} and Mg^{2+} were measured by atomic absorption spectrophotometry. K^+ and Na^+ were measured by flame photometry, while P was measured by the colorimetric method, and Al^{3+} was measured by titration. The TOC was determined by wet combustion with K^+ dichromate, and the TN was quantified in the soil samples submitted to sulfuric digestion and dosed by Kjedhal distillation. All analyses were performed according to methodologies described by Teixeira, Donagema, Fontana, and Teixeira (2017).

From the above results, the sum of bases (SB), potential cation exchange capacity (CECT), base saturation (V), aluminum saturation (m), and exchangeable sodium percentage (ESP) were calculated according to Teixeira et al. (2017).

We evaluated the P concentration that remained in the equilibrium solution after a certain period of contact with the soil in response to the application of P (P-rem). The P-rem was determined according to Alvarez V., Novais, Cantarutti, Teixeira, and Campos (2017). To determine the maximum P adsorption capacity (MPAC), the soil samples received doses of P based on the value of P-rem. Samples from each soil were saturated with solutions of increasing concentrations of P in $CaCl_2$ 0.01 mmol L^{-1}. Each soil layer received 11 doses of P (KH_2PO_4) with an interval according to the P-rem, defined by Alvarez and Fonseca (1990). Thus, adsorption curves were constructed relating the P-rem as a function of increasing doses of P. These curves established three regions with different inclinations: very inclined (region I), moderately inclined (region II) and slightly inclined (region III). We chose data from region II to not overestimate adsorption (region I) or underestimate adsorption (region III). The Langmuir isotherm (C/q = 1/ab+1/bC) was adjusted to data from region II to determine MPAC (b), expressed in mg cm^{-3}, and the constant (a), related to the adsorption energy (EA), expressed in (L mg^{-1})$^{-1}$.

P was fractionated using the method proposed by Chang and Jackson (1957), with modifications suggested by Kuo (1996). From this analysis, it was possible to determine soluble P (P-H_2O), extracted by NH_4Cl; P associated with Al (P-Al), extracted by NH_4F; P associated with Fe (P-Fe), extracted by NaOH; and P associated with Ca (P-Ca), extracted by H_2SO_4. The addition of these extractors is carried out sequentially. Pi Total (Pi-Total) was calculated as the sum of the inorganic fractions of P.

Mineralogical analysis

The mineralogy of the clay fraction was determined by X-ray diffraction (Moore & Reynolds, 1997). The readings of the samples were performed on a diffractometer equipped with a copper tube using CuKα radiation operated at 20 mA and 40 kV.

Crystalline and low-crystalline Fe forms (Fe-DCB) were extracted with sodium dithionite-citrate-bicarbonate (DCB). The extraction of low-crystallinity Fe forms (Fe-AO) was performed with ammonium oxalate (AO). The crystalline Fe forms (Fe-crystalline) were obtained by the difference between the forms extracted by DCB and AO. All analyses were performed according to methodologies described by Cornell and Schwertmann (2003).

Statistical analyses

Data were analyzed by multivariate statistics through principal component analysis (PCA) to select the PBC indicators most related to the different soil types and to identify similar groups (Shiker, 2012). Pearson's linear correlation coefficients were determined between the forms of P and characteristics of the soils. ASSISTAT 7.7 software was used to perform the statistical analysis (Silva & Azevedo, 2016).

Results and discussion

Physicochemical and mineralogical characteristics of soils

The VRha$_1$, VRha$_2$ and FRgr$_2$ soils showed the highest clay contents, with values ranging from 450 to 567 g kg^{-1}, categorized as the clay textural class (Table 2). The higher clay content found in VRha$_2$ (532 g kg^{-1}) can be attributed to the influence of the parent material (Santos et al., 2019), since it originates from clay.

Lower pH values in KCl compared to pH in water resulted in a negative ΔpH (Table 2), showing a predominance of negative charges in all soils, except for FRac, which in the subsurface layer showed positive charges, indicating its acric character. For the pH values in water, the pH values in KCl varied between 8.54 and 4.16. The higher pH value found in VRha$_1$ can be attributed to limestone, a parent material of great influence on soil neutralization reactions.

The highest Na$^+$ content was found in VRha$_2$, especially in the subsurface layer (1.19 cmol$_c$ dm^{-3}) (Table 2), which resulted in the highest saturation value for this element (3%) compared to the other soils. A similar result was found by Zhang, Zhan, He, Feng, and Kang (2018) in calcareous saline-sodic soil from China.

Only Ferralsols presented Al^{3+} in the exchange complex, especially FRgr$_2$, which had levels varying from 1.83 to 2.02 cmol$_c$ dm^{-3} in the 0-20 and 20-40 cm layers, respectively, which were reflected by a high saturation of aluminum (89 and 88% at the respective depths) (Table 2).

Table 2. Physical-chemical characteristics of the soils.

Depth cm	Clay g kg^{-1}	pH H$_2$O	KCl	ΔpH	Ca^{2+}	Mg^{2+}	K$^+$	Na$^+$	Al^{3+}	(H+Al)	SB	CEC$_T$	V	m	ESP	TOC	TN	P	P-rem	MPAC
							cmol$_c$ dm^{-3}							%		g kg^{-1}		mg dm^{-3}	mg L^{-1}	mg cm^{-3}
								VRha$_1$ – Juazeiro - BA												
0-20	450	8.54	7.25	-1.29	44.52	1.19	0.33	0.15	0.00	0.74	46.19	46.93	98	0	0	5.64	0.17	1.54	26.00	0.69
20-40	452	8.53	7.03	-1.50	45.45	1.01	0.13	0.23	0.00	0.66	46.82	47.48	98	0	0	4.50	0.14	1.13	25.79	0.68
								VRha$_2$ – Souza - PB												
0-20	516	7.54	5.78	-1.76	26.67	7.42	1.00	0.56	0.00	1.79	35.65	37.44	95	0	1	5.69	0.19	23.03	32.91	0.34
20-40	532	7.96	6.12	-1.84	28.90	6.96	0.78	1.19	0.00	1.65	37.83	39.48	95	0	3	4.14	0.10	23.58	32.17	0.46
								CMle – Baraúna - RN												
0-20	407	7.21	6.14	-1.07	7.63	0.91	0.87	0.04	0.00	1.10	9.45	10.55	89	0	0	14.83	0.38	1.88	37.29	0.35
20-40	448	7.21	5.85	-1.36	5.81	0.29	1.12	0.04	0.00	1.35	7.26	8.61	84	0	0	6.58	0.19	1.03	31.61	0.41
								FRac – Rio Verde - GO												
0-20	407	5.98	5.00	-0.98	1.63	0.46	0.29	0.00	0.05	2.12	2.38	7.30	32	2	0	20.02	0.25	3.25	29.38	0.64
20-40	476	5.55	5.87	0.32	0.14	0.06	0.12	0.00	0.78	4.92	0.32	2.44	13	70	0	4.42	0.24	0.71	5.08	1.67
								FRgr$_1$ – Bom Jesus - PI												
0-20	141	5.48	3.71	-1.77	0.07	0.02	0.03	0.03	1.28	6.82	0.15	6.97	2	89	0	17.8	0.20	2.70	47.34	0.13
20-40	141	5.02	4.15	-0.87	0.06	0.00	0.01	0.02	0.72	3.41	0.09	3.50	2	88	0	7.14	0.11	1.32	46.32	0.10
								FRgr$_2$ – Ribeirão - PE												
0-20	468	4.31	3.52	-0.79	0.15	0.2	0.09	0.03	1.83	6.52	0.54	7.06	7	77	0	32.53	0.36	2.58	25.40	0.68
20-40	567	4.16	3.68	-0.48	0.22	0.04	0.03	0.01	2.02	12.18	0.23	12.41	2	89	0	14.9	0.29	1.25	18.20	0.71
								FReu– Petrolina - PE												
0-20	141	6.37	5.47	-0.90	2.81	0.32	0.22	0.03	0.05	1.65	3.38	5.03	67	1	0	9.35	0.21	26.97	59.27	0.19
20-40	141	5.66	4.79	-0.87	0.94	0.17	0.14	0.03	1.10	1.87	1.28	3.15	40	46	1	3.06	0.15	3.66	57.58	0.22

VRha$_1$, Haplic Vertisol (Calcaric); VRha$_2$, Haplic Sodic Vertisol; CMle, Calcaric Leptic Cambisol; FRac, Geric Acric Ferralsol; FRgr$_1$, Geric Ferralsol (Dystric); FRgr$_2$, Geric Ferralsol (Dystric); FReu, Ferralsol (Eutric, Loamic); ΔpH = pH (KCl) − pH (water). The pH analysis in KCl shows the reserve pH and the pH analysis in water shows the active pH; SB, sum of bases; CEC$_T$, potential cation exchange capacity; V, base saturation; m, aluminum saturation; ESP, exchangeable sodium percentage; TOC, total organic carbon; TN, total nitrogen; P-rem, P-remaining; MPAC, maximum P adsorption capacity. The coefficient of variation of the data ranged from 3.7% (pH) to 23.5% (P available).

The highest contents of Ca^{2+} and Mg^{2+} were found in the Vertisols, with values varying between 26.67 and 45.45 $cmol_c$ dm^{-3} for Ca^{2+} and 1.01 and 7.42 $cmol_c$ dm^{-3} for Mg^{2+}, contributing to a high base sum value and base saturation (Table 2). High contents of basic cations in Vertisols have been verified in the literature (Pal, Wani, & Sahrawat, 2012), which can be attributed to the nature of the parent material of these soils. Ca^{2+} cations predominate when the parent material is sedimentary, and Mg^{2+} cations predominate when the parent material is igneous (Tamfuh et al., 2018).

The levels of soil available P showed values ranging from 0.71 mg dm^{-3} to 26.97 mg dm^{-3} (Table 2). In general, the highest levels of P are found on the surface due to the presence of organic matter (confirmed by the highest levels of TOC), since P is part of the structure of organic molecules (Tipping, Somerville, & Luster, 2016).

Values of P available in VRha$_2$ greater than 23 mg dm^{-3} (Table 2) may be overestimated, which may have occurred due to the capacity of Mehlich-1 to solubilize calcium phosphates. In this situation, the extractor recovers the fraction of P not accessible by the plant (P-Ca), overestimating the available contents of this element. Braun et al. (2019), in six different sites within long-term Swedish soil fertility experiments, observed better performance of the Olsen extractor in calcareous and noncalcareous soils than the acid extractor. The authors reported that the Olsen extractor showed uniform performance and extracted less nonlabile P than the acid extractor. However, the lower P recovery by Mehlich-1 in soils with high clay content, high MPAC, and low P-rem can be attributed to the sensitivity of Mehlich-1 to the PBC of the soil, such as in the subsurface layer of FRac (0.71 mg dm^{-3}). In more buffered soils, the pH of the Mehlich-1 extractor is raised to values close to that of the soil, decreasing its extraction capacity (Novais et al., 2015).

Fe extracted with sodium ditionite-citrate-bicarbonate (Fe-DCB) and Fe extracted with ammonium oxalate (Fe-AO) varied from 9.35 to 146.07 and from 0.44 to 6.99 g kg$^-$, respectively (Table 3). The levels of Fe-DCB were higher in the FRac (119 and 146 g kg^{-1} in the 0-20 and 20-40 cm layers, respectively). This result is consistent with the basaltic parent material, which presents high levels of Fe, as described by Owonubi (2020).

The VRha$_1$, VRha$_2$, and FReu soils showed low levels of Fe-DCB, which can be attributed to the parent material, limestone, clay and sedimentary cover, respectively, being responsible for low levels of Fe. In addition, the high pH value of these soils may have favored the low solubility of Fe.

Crystalline Fe values ranged from 8.91 to 139.08 g kg^{-1}, while low-crystalline ferric minerals (Fe-AO) showed values from 0.44 to 6.99 g kg^{-1} (Table 3). This provided a low Fe-AO:Fe-DCB ratio, highlighting the predominance of ferric minerals with high crystallinity, such as hematite and goethite. The goethite was found in most soils (Table 3).

Table 3. Minerals of clay fraction of the soils, Fe oxide content extracted by dithionite-citrate-bicarbonate (DCB) (Fe-DCB) and ammonium oxalate (AO) (Fe-AO), as well as Fe-crystalline [(Fe-DCB) - (Fe-AO)] and the relationship Fe-AO/Fe-DCB.

Soil	Depth	Minerals	Fe-DCB	Fe-AO	Fe-crystalline	Fe-AO/Fe-DCB
	cm			g kg^{-1}		
VRha$_1$	0-20	Ct, Mi	20.49 ± 1.02	1.59 ± 0.05	18.90 ± 0.97	0.07 ± 0.003
	20-40	Ct, Mi	18.63 ± 1.30	1.74 ± 0.09	16.89 ± 0.94	0.09 ± 0.004
VRha$_2$	0-20	Es, Mi	16.93 ± 1.19	6.74 ± 0.27	10.19 ± 0.92	0.40 ± 0.022
	20-40	Es, Mi	19.82 ± 2.58	5.74 ± 0.29	14.08 ± 2.29	0.30 ± 0.017
CMle	0-20	Mi, Ct, Gh	60.27 ± 2.41	0.79 ± 0.04	59.48 ± 2.37	0.01 ± 0.001
	20-40	Mi, Ct, Gh	67.14 ± 5.37	0.64 ± 0.04	66.5 ± 5.33	0.01 ± 0.001
FRac	0-20	Ct, Gb, Gh, Hm	119.01 ± 10.71	4.56 ± 0.09	114.45 ± 10.62	0.04 ± 0.001
	20-40	Ct, Gb, Gh, Hm	146.07 ± 16.07	6.99 ± 0.28	139.08 ± 15.79	0.05 ± 0.002
FRgr$_1$	0-20	Mi, Ct, Gh	23.18 ± 2.78	1.01 ± 0.03	22.17 ± 2.75	0.04 ± 0.002
	20-40	Mi, Ct, Gh	46.57 ± 3.26	0.81 ± 0.03	45.76 ± 3.23	0.01 ± 0.001
FRgr$_2$	0-20	Ct, Gh, Gb	66.80 ± 7.35	7.59 ± 0.38	59.21 ± 6.97	0.11 ± 0.013
	20-40	Ct, Gh, Gb	71.17 ± 2.85	7.03 ± 0.49	64.14 ± 2.36	0.10 ± 0.010
FReu	0-20	Mi, Ct, Gh	16.30 ± 0.98	0.77 ± 0.03	15.53 ± 0.95	0.04 ± 0.002
	20-40	Mi, Ct, Gh	9.35 ± 0.84	0.44 ± 0.01	8.91 ± 0.83	0.04 ± 0.002

VRha$_1$, Haplic Vertisol (Calcaric); VRha$_2$, Haplic Sodic Vertisol; CMle, Calcaric Leptic Cambisol; FRac, Geric Acric Ferralsol; FRgr$_1$, Geric Ferralsol (Dystric); FRgr$_2$, Geric Ferralsol (Dystric); FReu, Ferralsol (Eutric, Loamic); Ct, kaolinite; Mi, mica; Es, smectite; Gh, goethite; Gb, gibbsite; Hm, hematite.

The soils differed regarding the levels of total inorganic P (Pi-Total), with values ranging from 11.94 to 34.75 mg kg^{-1} (Table 4). The highest levels of this fraction were observed in VRha$_1$ and VRha$_2$, with 34.75 and 26.75 mg kg^{-1}, respectively. The Pi-Total contents differentiated between soils can be attributed to the clay content, their parent material and the environmental conditions in which each soil is found (Antoniadis, Koliniati, Efstratiou, Golia, & Petropoulos, 2016; Redel et al., 2016). Rocha, Duda, Nascimento, and Ribeiro

(2005), studied the fractionation of organic and inorganic P in soils of Fernando de Noronha Island and reported that the high levels of P observed were due to parent material volcanic and guano deposits. Nishigaki et al. (2018), in another study carried out with soils from Tanzania, demonstrated that the forms of P differed according to the different geological conditions of the studied sites and soil properties. Additionally, Souza Júnior et al. (2012) showed that soils with the highest levels of Pi-Total were those with the highest clay contents.

Table 4. P contents of inorganic P fraction of the soils.

Soil	Depth cm	Pi-Total	P-H_2O	P-Al	P-Fe	P-Ca
				mg kg^{-1}		
VRha$_1$	0-20	34.75 ± 3.88	8.41 ± 1.62 (24)	2.05 ± 1.33 (6)	5.51 ± 0.29 (16)	18.78 ± 0.64 (54)
	20-40	26.83 ± 3.14	7.77 ± 0.65 (29)	1.85 ± 0.33 (7)	5.06 ± 0.61 (19)	12.15 ± 1.55 (45)
VRha$_2$	0-20	26.75 ± 3.95	7.51 ± 0.77 (28)	0.34 ± 0.14 (1)	2.40 ± 0.34 (9)	16.5 ± 2.70 (62)
	20-40	27.46 ± 2.35	7.38 ± 0.73 (27)	0.34 ± 0.17 (1)	1.24 ± 0.41 (5)	18.5 ± 1.04 (67)
CMle	0-20	11.94 ± 1.20	7.77 ± 0.49 (65)	0.54 ± 0.12 (5)	1.24 ± 0.29 (10)	2.39 ± 0.30 (20)
	20-40	14.20 ± 3.01	7.90 ± 0.42 (56)	0.14 ± 0.05 (1)	4.09 ± 1.16 (29)	2.07 ± 1.38 (15)
FRac	0-20	17.58 ± 1.71	6.62 ± 0.30 (38)	0.24 ± 0.10 (1)	9.06 ± 1.01 (52)	1.66 ± 0.30 (9)
	20-40	17.83 ± 2.31	8.15 ± 0.89 (46)	2.46 ± 0.33 (14)	4.09 ± 0.29 (23)	3.13 ± 0.80 (18)
FRgr$_1$	0-20	12.68 ± 2.77	7.04 ± 0.87 (56)	1.65 ± 0.65 (13)	1.60 ± 0.82 (13)	2.39 ± 0.43 (19)
	20-40	15.24 ± 1.95	7.77 ± 0.65 (51)	1.35 ± 0.95 (9)	4.92 ± 0.17 (32)	1.20 ± 0.18 (8)
FRgr$_2$	0-20	15.90 ± 2.82	6.74 ± 0.65 (42)	0.14 ± 0.02 (1)	5.42 ± 1.80 (34)	3.60 ± 0.35 (23)
	20-40	14.30 ± 1.21	5.33 ± 0.73 (37)	4.50 ± 0.08 (31)	0.89 ± 0.10 (6)	3.58 ± 0.30 (24)
FReu	0-20	14.23 ± 2.50	6.74 ± 1.06 (47)	2.05 ± 0.47 (14)	2.04 ± 0.34 (14)	3.40 ± 0.63 (24)
	20-40	15.54 ± 2.47	8.41 ± 1.28 (54)	1.45 ± 0.23 (9)	3.38 ± 0.41 (22)	2.30 ± 0.55 (15)

VRha$_1$, Haplic Vertisol (Calcaric); VRha$_2$, Haplic Sodic Vertisol; CMle, Calcaric Leptic Cambisol; FRac, Geric Acric Ferralsol; FRgr$_1$, Geric Ferralsol (Dystric); FRgr$_2$, Geric Ferralsol (Dystric); FReu, Ferralsol (Eutric, Loamic); P-H_2O, P-Al, P-Fe and P-Ca, fractions of inorganic P (Chang & Jackson, 1957); Pi-Total = P-H_2O + P-Al + P-Fe + P-Ca. Values in parentheses are the percentage of the contribution of each fraction of P to the Pi-Total.

The soluble P fraction (P-H_2O) had the highest P content among the other fractions, except for VRha$_1$ and VRha$_2$, which presented the highest P content in the P-Ca fraction, and FRac, which presented 52% Pi in the P-Fe fraction in the surface layer (Table 4). The FReu and CMle soils showed the highest P content in the soluble fraction, representing 54% and 65% of the Pi-Total, respectively (Table 4). Low levels of soluble P in highly weathered soils are commonly reported in the literature (Souza Júnior et al., 2012; Penn & Camberato, 2019). However, this will not always occur, since P fixation is largely dependent on the mineralogical constituents of the clay fraction of soils and their consequent interaction with P (Fink et al., 2016a).

The P-Al and P-Fe fractions were, respectively, more significant in the 20-40 cm layer of FRgr$_2$ and in the 0-20 cm layer of FRac (Table 4), which are very weathered soils with a high clay content and a low pH (Table 2). Additionally, the FRac, originating from basalt, presented high levels of Fe-DCB (146.07 g kg^{-1}) (Table 3), which may have contributed to a greater precipitation of this element with P, as verified by Antoniadis et al. (2016) in central Greece soils. This is in accordance with the correlation analysis, since Fe-DCB and P-rem correlated negatively (r = - 0.65*) (Table 5).

Table 5. Pearson's linear correlation coefficient between soil P fractions and phosphate buffer capacity (PBC) indicators.

	Pi-Total	P-H_2O	P-Al	P-Fe	P-Ca	Clay	P-rem	MPAC	AE	Fe-AO	Fe-DCB	TOC
Pi-Total	-	0.324^{ns}	-0.123^{ns}	0.266^{ns}	0.934^{ns}	0.459*	-0.315^{ns}	0.219^{ns}	-0.330^{ns}	0.220^{ns}	-0.327^{ns}	-0.334^{ns}
P-H_2O	-	-	-0.574*	0.212^{ns}	0.215^{ns}	-0.274^{ns}	0.186^{ns}	-0.016^{ns}	-0.234^{ns}	-0.473*	-0.191^{ns}	-0.481*
P-Al	-	-	-	-0.145^{ns}	-0.175^{ns}	0.106^{ns}	-0.310^{ns}	0.363^{ns}	0.174^{ns}	0.361^{ns}	0.133^{ns}	0.323^{ns}
P-Fe	-	-	-	-	-0.060^{ns}	0.088^{ns}	-0.259^{ns}	0.304^{ns}	-0.007^{ns}	0.054^{ns}	0.409^{ns}	0.236^{ns}
P-Ca	-	-	-	-	-	0.479*	-0.219^{ns}	0.065^{ns}	-0.340^{ns}	0.222^{ns}	-0.473*	-0.412^{ns}
Clay	-	-	-	-	-	-	-0.839***	0.582*	0.259^{ns}	0.697**	0.339^{ns}	0.058^{ns}
P-rem	-	-	-	-	-	-	-	-0.869***	-0.528*	-0.686**	-0.650*	-0.091^{ns}
MPAC	-	-	-	-	-	-	-	-	0.549*	0.587*	0.719**	-0.027^{ns}
AE	-	-	-	-	-	-	-	-	-	0.540*	0.705**	0.298^{ns}
Fe-AO	-	-	-	-	-	-	-	-	-	-	0.448°	0.320^{ns}
Fe-DCB	-	-	-	-	-	-	-	-	-	-	-	0.299^{ns}
TOC	-	-	-	-	-	-	-	-	-	-	-	-

P-H_2O, P-Al, P-Fe and P-Ca, fractions of inorganic P (Chang & Jackson, 1957); Pi-Total = P-H_2O + P-Al + P-Fe + P-Ca; P-rem, P-remaining; MPAC, maximum P adsorption capacity; AE, Adsorption energy; Fe-AO, Fe extracted with ammonium oxalate; Fe-DCB, Fe extracted with sodium dithionite-citrate-bicarbonate; TOC, Total organic carbon. $^\circ$, *, ** and *** significant at 10, 5, 1 and 0.1%, respectively. ^{ns} Not significant.

The highest P contents of the soils VRha$_1$ and VRha$_2$ were found in the P-Ca fraction, with percentage values in the surface layer at 54 and 62%, respectively (Table 4). This is consistent with the high levels of Ca in these soils

(Table 2). Souza Júnior et al. (2012) observed a similar result in soils of different weathering degrees, where neutral to alkaline pH soils had P-Ca as the predominant fraction, representing on average 55% of the Pi-Total.

Relationships between indicators of soil phosphate buffer capacity and the inorganic P fractions

For a better understanding of the P fractions, as well as the factors that interfere with the P availability in the soil, correlations were made between the P fixation indicators and the inorganic P fractions. In general, the soil P fractions did not correlate with the PBC indicators (Table 5). The P-H_2O fraction (readily available P) showed a negative correlation with the P-Al fraction (Table 5), suggesting that the minerals responsible for P fixation were those associated with aluminum, such as gibbsite, which was found in the soils FRac and $FRgr_2$ (Table 3). The presence of ferric minerals, such as goethite and hematite, found in most soils did not significantly influence P fixation (Table 3).

The relationship between gibbsite, goethite and hematite minerals and P fixation is widely discussed in the literature (Fink et al., 2016b; Gérard, 2016; Fang, Chi, He, Huang, & Chen, 2017; Abdala et al., 2020; Oliveira et al., 2020). Wei, Tan, Liu, Zhao, and Weng (2014) showed that gibbsite was responsible for restricting the desorption of labile P in soil. Gypser, Hirsch, Schleicher, and Freese (2018) reported the quality of gibbsites as an indicator of P fixation.

Another negative correlation of the P-H_2O fraction was with TOC (Table 5). Shariatmadari, Shirvani, and Dehghan (1977), studied the availability of organic and inorganic P fractions in calcareous soils and reported that the TOC content was the soil property that more affected the size of the P fractions. Shah, Rai, and Azis (2019) found that P availability was positively correlated with TOC in acidic soils from northwestern India. The P availability from the soils in our study was more correlated with the levels of clay, P-rem and the different forms of Fe (Fe-DCB and Fe-AO) (Table 5). TOC levels were very low, as is common in soils in Northeast Brazil (Fidalgo et al., 2007). The negative correlation may have been a consequence of these low levels, having little influence on the availability of P ($p < 10\%$).

The clay content of the soils correlated with the P-rem (Table 5). The P-rem analysis, as an estimator of the PBC of soils, replacing the clay content, emerged with the hypothesis that P fixation is better related to the quality of the clay and not just to the amount (Eriksson et al., 2016; Fink et al., 2016a). Therefore, the relationship between these two soil phosphate buffer estimators would be expected to be low. In this study, the P-rem contents ranged from 5.08 to 59.27 mg L^{-1}, and clay contents ranged from 141 to 567 g kg^{-1} (Table 2). The relationship between the variables was very significant (r = -0.839 ***) (Table 5), suggesting that the determination of one of these indicators can be used to adequately estimate the other, even on soils with different mineralogical compositions. Rogeri, Gianello, Bortolon, and Amorim (2016) showed that this estimate was better in soils with higher clay contents.

However, the best estimator of the PBC of soils was P-rem because it showed a better correlation with MPAC, AE, Fe-AO, and Fe-DCB (Table 5). Other studies (Novais et al., 2015; Alovisi et al., 2020) also found that the P-rem better estimated the MPAC and PBC. Rogeri et al. (2016) suggested a routine laboratory assay for soil fertility in Brazil, performing P-rem analysis to estimate PBC is more advantageous than clay determination due to its greater predictive capacity.

The levels of Fe oxides [(Fe-AO and Fe-DCB)] also correlated with MPAC and AE (Table 5), suggesting that they are good indicators of the PBC of these soils. Several studies have confirmed the contribution of Fe oxides in the P fixation process, especially those of low crystallinity and with high load imbalance (Fink et al., 2016b; Camêlo et al., 2017), normally exceeding the contribution of kaolinite, illite and montmorillonite. Wei et al. (2014) compared the phosphate adsorption between kaolinite and goethite and reported that the maximum adsorption capacity of goethite was approximately 300 mmol g^{-1}, which was six times greater than that of kaolinite, which showed the ability to adsorb P at approximately 50 mmol g^{-1}.

Grouping of soils of different mineralogical compositions according to the phosphate buffer capacity indicators

We studied how the soils were grouped in relation to the P fixation indicators by principal component analysis (PCA) (Figure 2). In the superficial layer (0-20 cm deep), four groups of soils were formed: i) FRac and $FRgr_2$ were the soils most influenced by PBC indicators; ii) Vertisols $VRha_1$ and $VRha_2$ were influenced by P-Ca and clay content; iii) CMle and $FRgr_1$ were little influenced; and iv) FReu did not group (Figure 2A). The soils FRac and $FRgr_2$ are kaolinitic, with the presence of Al and Fe oxides; the Vertisols have much 2:1 clay (mica), with $VRha_2$ presenting more smectite and $VRha_1$ more kaolinite; and FReu, CMle and $FRgr_1$ are

kaolinitic with the presence of goethite (Table 3). This group had the lowest fixation of P and is widely found in agricultural enterprises in Northeast Brazil (Figure 1).

The soils were better grouped in the subsurface layer (20-40 cm deep) (Figure 2B), which may have occurred due to the decrease in the organic matter content (Table 2). The soils FRac and FRgr$_2$ showed a mineralogical difference, despite being kaolinitic. FRac showed more gibbsites than FRgr$_2$, in addition to expressing hematite peaks. Vertisols showed mineralogical differences, showing more smectite in VRha$_1$ and kaolinite in VRha$_2$. FReu, CMle, and FRgr$_1$ grouped even more in this layer due to the greater mineralogical similarity (Table 3).

Principal component analysis (PCA) showed that many soils (VRha$_1$, VRha$_2$, FRha, FRgr$_1$, and CMle) were less influenced by the PBC indicators in the superficial layer (Figure 2A). This may be related to the ability of organic compounds to block hydroxyls exposed on the surface of clay minerals, increasing P availability (Kurnain, 2016; Maranguit, Guilaume, & Kuzyakov, 2017; Maharjan, Maranguit, & Kuzyakov, 2018; Yang, Chen, & Yang, 2019).

The isolation of FRac from other soils (Figure 2) results from the high content of Fe oxides in its mineralogical composition. The Fe-DCB and Fe-AO of the FRac were 119.01 and 4.56 g kg^{-1} (0-20 cm deep) and 146.07 and 6.99 g kg^{-1} (20-40 cm deep), respectively. The Fe-AO/Fe-DCB ratio was low, indicating a predominance of Fe crystals, such as hematite, detrimental to the low crystallinity of Fe oxides (Table 3).
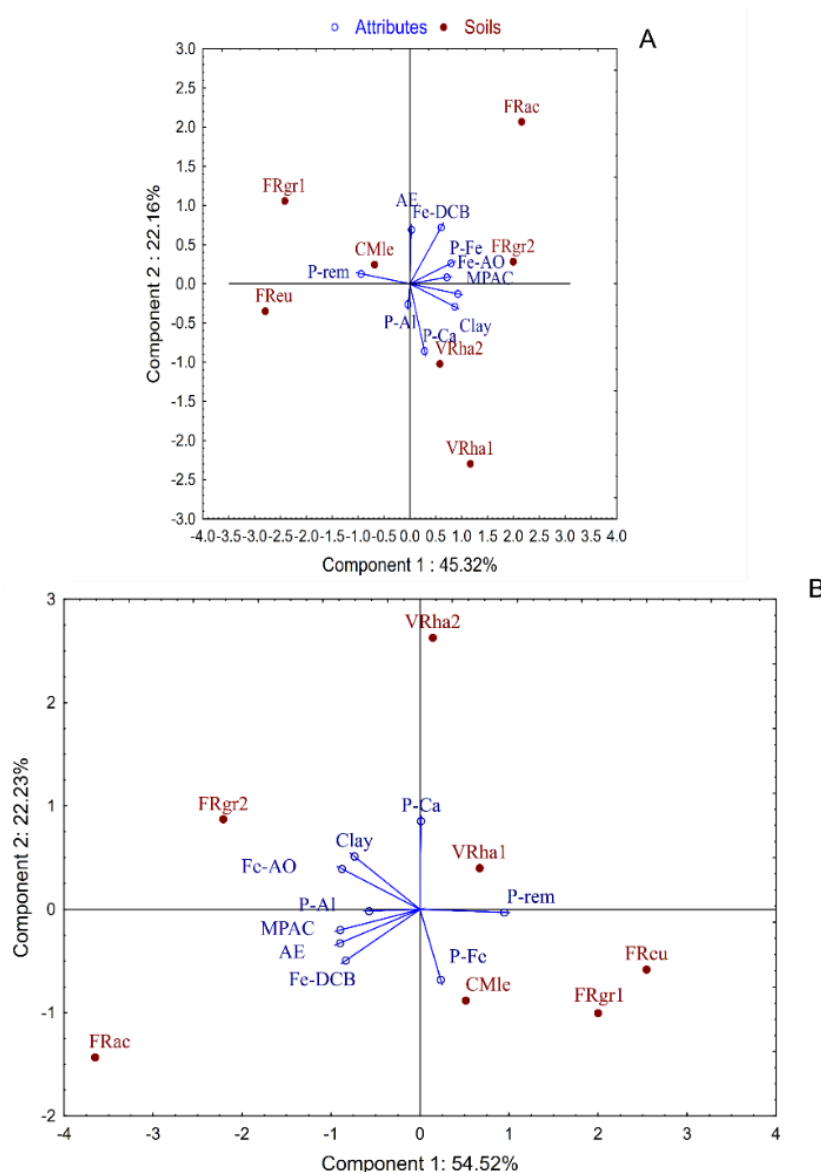
Figure 2. Principal component analysis (PCA) that relates the type of the soil with indicators of the phosphate buffer capacity (PBC) in the layers 0-20 cm (A) and 20-40 cm (B) deep. VRha$_1$, Haplic Vertisol (Calcaric); VRha$_2$, Haplic Sodic Vertisol; CMle, Calcaric Leptic Cambisol; FRac, Geric Acric Ferralsol; FRgr$_1$, Geric Ferralsol (Dystric); FRgr$_2$, Geric Ferralsol (Dystric); FReu, Ferralsol (Eutric, Loamic); P-rem, P-remaining; MPAC, maximum P adsorption capacity; AE, Adsorption energy; Fe-AO, Fe extracted with ammonium oxalate; Fe-DCB, Fe extracted with sodium dithionite-citrate-bicarbonate; P-Ca, P associated to Ca; P-Al, P associated to Al; and P-Fe, P associated to Fe.

The P fractions, PBC indicators and the distribution of the soils revealed the strong relationship between FRac and MPAC, AE, Fe-DCB, and P-Al; FRgr$_2$ was highly related to Fe-AO, clay, and P-Al; VRha$_1$ and VRha$_2$ were related to P-Ca and P-rem; FReu, CMle, and FRgr$_1$ were related to P-Fe and P-rem (Figure 2). These groups allowed us to conclude that the soils with the highest P fixation rates were those that were related to P-Al; the soils with moderate fixation were those that were related to P-Ca; and the ones with the lowest fixation rates were those related to P-Fe.

Conclusion

The minerals of aluminum contributed the most to P fixation within our study, such as gibbsite, which was found in the soils FRac and FRgr$_2$. P-rem was the best estimator of PBC. The soils with high, moderate and low rates of P fixation showed high amounts of P-Al, P-Ca, and P-Fe fractions, respectively. The results showed that P fixation is influenced by the fractions of P within the soil, suggesting that the efficiency of phosphate fertilizers in tropical soils depends on the mineralogy of the clay fraction.

References

Abdala, D. B., Gatiboni, L. C., Schimitt, D. E., Mumbach, G. L., Dall'Orsoletta, D. J., Bonfada, E. B., & Veiga, M. (2020). Phosphorus speciation and iron mineralogy in an oxisol after 11 years of pig slurry application. *Science of the Total Environment, 743*, e140487. DOI: https://doi.org/10.1016/j.scitotenv.2020.140487

Abdala, D. B., Silva, I. R., Vergutz, L., & Sparks, D. L. (2015). Long-term manure application effects on phosphorus speciation, kinetics and distribution in highly weathered agricultural soils. *Chemosphere, 119*, 504-514. DOI: https://doi.org/10.1016/j.chemosphere.2014.07.029

Alovisi, A. M. T., Cassol, C. J., Nascimento, J. S., Soares, N. B., Silva Junior, I. R., Silva, R. S., & Silva, J. A. M. (2020). Soil factors affecting phosphorus adsorption in soil of Cerrado, Brazil. *Geoderma Regional, 22*, e00298. DOI: https://doi.org/10.1016/j.geodrs.2020.e00298

Alvares, C. A., Stape, J. L., Sentelhas, P. C., Gonçalves, J. L. M., & Sparovek V. (2013). Köppen's climate classification map for Brazil. *Meteorologische Zeitschrift, 22*(6), 711-728. DOI: https://doi.org/10.1127/0941-2948/2013/0507

Alvarez, V., V. H., & Fonseca, D. M. (1990). Definição de doses de fósforo para determinação da capacidade máxima de adsorção de fosfatos e para ensaios em casa de vegetação. *Revista Brasileira de Ciência do Solo, 14*(1), 49-55.

Alvarez V., V. H., Novais, R. F., Cantarutti, R. B., Teixeira, P. C., & Campos, D. V. B. (2017). Fósforo remanescente. In P. C. Teixeira, G. K. Donagemma, A. Fontana, & W. G. Teixeira (Eds.), *Manual de métodos de análise de solos* (p. 337-342). Rio de Janeiro, RJ: Embrapa.

Antoniadis, V., Koliniati, R., Efstratiou, E., Golia, E., & Petropoulos, S. (2016). Effect of soils with varying degree of weathering and pH values on phosphorus sorption. *Catena, 139*, 214-219. DOI: https://doi.org/10.1016/j.catena.2016.01.008

Braun, S., Warrinnier, R., Börjesson, G., Ulén, B., Smolders, E., & Gustafsson, J. P. (2019). Assessing the ability of soil tests to estimate labile phosphorus in agricultural soils: evidence from isotopic exchange. *Geoderma, 337*, 350-358. DOI: https://doi.org/10.1016/j.geoderma.2018.09.048

Camêlo, D. L., Ker, J. C., Fontes, M. P. F., Corrêa, M. M., Costa, A. C. S., & Melo, V. F. (2017). Pedogenic iron oxides in iron-rich oxisols developed from mafic rocks. *Revista Brasileira de Ciência do Solo, 41*, 1-16. DOI: https://doi.org/10.1590/18069657rbcs20160379

Chang, S. C., & Jackson, M. L. (1957). Fractionation of soil phosphorus. *Soil Science, 84*(2), 133-144. DOI: https://doi.org/10.1097/00010694-195708000-00005

Christophe, T., Bourg, I. C., Steefel, C. I., & Bergaya, F. (2015). Surface properties of clay minerals. *Developments in Clay Science, 6*, 5-31. DOI: https://doi.org/10.1016/B978-0-08-100027-4.00001-2

Cornell, R. M., & Schwertmann, U. (2003). *The iron oxides: Structure, properties, reactions, occurrences and uses*. Weinheim, DE: John Wiley & Sons.

Eriksson, A. K., Hesterberg, D., Klysubun, W., & Gutafsson, J. P. (2016). Phosphorus dynamics in Swedish agricultural soils as influenced by fertilization and mineralogical properties: Insights gained from batch

experiments and XANES spectroscopy. *Science of the Total Environment*, *566-567,* 1410-1419. DOI: https://doi.org/10.1016/j.scitotenv.2016.05.225

Fang, H., Chi, Z., He, G., Huang, L., & Chen, M. (2017). Phosphorus adsorption onto clay minerals and iron oxide with consideration of heterogeneous particle morphology. *Science of the Total Environment, 605-605*, 357-367. DOI: https://doi.org/10.1016/j.scitotenv.2017.05.133

Fidalgo, E. C. C., Benites, V. M., Machado, P. L. O. A., Madari, B. E., Coelho, M. R., Moura, I. B., & Lima, C. X. (2007). *Estoque de carbono nos solos do Brasil*. Rio de Janeiro, RJ: Embrapa.

Fink, J. R., Inda Junior, A. V., Bavaresco, J., Barrón, V., Torrent, J., & Bayer, C. (2016a). Adsorption and desorption of phosphorus in subtropical soils as affected by management system and mineralogy. *Soil & Tillage Research*, *155*, 62-68. DOI: https://doi.org/10.1016/j.still.2015.07.017

Fink, J. R., Inda Junior, A. V., Tiecher, T., & Barrón, V. (2016b). Iron oxides and organic matter on soil phosphorus availability. *Ciência e Agrotecnologia*, *40*(4), 369-379. DOI: https://doi.org/10.1590/1413-70542016404023016

Gérard, F. (2016). Clay minerals, iron/aluminum oxides, and their contribution to phosphate sorption in soils - A myth revisited. *Geoderma*, *262*, 213-226. DOI: https://doi.org/10.1016/j.geoderma.2015.08.036

Gypser, S., Hirsch, F., Schleicher, A. M., & Freese, D. (2018). Impact of crystalline and amorphous iron and aluminum hydroxides on mechanisms of phosphate adsorption and desorption. *Journal of Environmental Sciences, 70*, 175-189. DOI: https://doi.org/10.1016/j.jes.2017.12.001

Instituto Nacional de Meteorologia [INMET]. (2020). *Climate monitoring*. Retrieved on May 25, 2020 from http://www.inmet.gov.br/portal/index.php?r=clima/normaisclimatologicas

IUSS Working Group WRB. (2014). *World reference base for soil resources 2014. International Soil Classification System for Naming Soils and Creating Legends for Soil Maps*. Rome, IT: FAO.

Khawmee, K., Suddhiprakarn, A., Kheoruenromne, I., & Singh, B. (2013). Surface charge properties of kaolinite from Thai soils. *Geoderma, 192*(1), 120-131. DOI: https://doi.org/10.1016/j.geoderma.2012.07.010

Kuo, S. (1996). Phosphorus. In J. M. Bigham (Ed.), *Methods of soil analysis: Chemical methods* (p. 869-920). Madison, US: American Society of Agronomy.

Kurnain, A. (2016). Inhibition of phosphorus adsorption to goethite and acid soil by organic matter. *International Journal of Soil Science*, *11*(3), 87-93. DOI: https://doi.org/10.3923/ijss.2016.87.93

Nishigaki, T., Sugihara, S., Kobayashi, K., Hashimoto, Y., Kilasara, M., Tanaka, H., ... Funakawa, S. (2018). Fractionation of phosphorus in soils with different geological and soil physicochemical properties in southern Tanzania. *Soil Science and Plant Nutrition*, *64*(3), 291-299. DOI: https://doi.org/10.1080/00380768.2018.1436406

Novais, S. V., Mattiello, E. M., Vergutz, L., Melo, L. C. A., Freitas, I. F., & Novais, R. F. (2015). Loss of extraction capacity of Mehlich-1 and monocalcium phosphate as a variable of remaining P and its relationship to critical Levels of soil phosphorus and sulfur. *Revista Brasileira de Ciência do Solo*, *39*(4), 1079-1087. DOI: https://doi.org/10.1590/01000683rbcs20140551

Maharjan, M., Maranguit, D., & Kuzyakov, Y. (2018). Phosphorus fractions in subtropical soils depending on land use. *European Journal of Soil Biology, 87*, 17-24. DOI: https://doi.org/10.1016/j.ejsobi.2018.04.002

Maranguit, D., Guillaume, T., & Kuzyakov, Y. (2017). Land-use change affects phosphorus fractions in highly weathered tropical soils. *Catena, 149*(Part 1), 385-393. DOI: https://doi.org/10.1016/j.catena.2016.10.010

Moore, D. M., & Reynolds, R. C. (1997). *X-ray diffraction and the identification and analysis of clay mineral*. Oxford, UK: Oxford University Press.

Oliveira, J. S., Inda A. V., Barrón, V., Torrent, J., Tiecher, T., & Camargo, F. A. O. (2020). Soil properties governing phosphorus adsorption in soils of Southern Brazil. *Geoderma Regional, 22,* 1-39. DOI: https://doi.org/10.1016/j.geodrs.2020.e00318

Owonubi, A. (2020). Pedogenic forms of iron in soils developed from four parent materials. *Journal of Tropical Soils, 25*(1), 47-52. DOI: https://doi.org/10.5400/jts.2020.v25i1.47

Pal, D. K., Wani, S. P., & Sahrawat, K. L. (2012). Vertisols of tropical Indian environments: Pedology and edaphology. *Geoderma*, *189-190*, 28-49. DOI: https://doi.org/10.1016/j.geoderma.2012.04.021

Penn, C. J., & Camberato, J. J. (2019). A critical review on soil chemical processes that control how soil pH affects phosphorus availability to plants. *Agriculture*, *9*(6), 1-18. DOI: https://doi.org/10.3390/agriculture9060120

Redel, Y., Cartes, P., Demanet, R., Velásquez, G., Poblete-Grant, P., Bol, R., & Mora, M. L. (2016). Assessment of phosphorus status influenced by Al and Fe compounds in volcanic grassland soils. *Soil Science and Plant Nutrition*, *16*(2), 490-506. DOI: https://doi.org/10.4067/S0718-95162016005000041

Rocha, A. T., Duda, G. P., Nascimento, C. W. A., & Ribeiro, M. R. (2005). Fracionamento do fósforo e avaliação de extratores do P-disponível em solos da Ilha de Fernando de Noronha. *Revista Brasileira de Engenharia Agrícola e Ambiental, 9*(2), 178-184. DOI: https://doi.org/10.1590/S1415-43662005000200005

Rogeri, D. A., Gianello, C., Bortolon, L., & Amorim, M. B. (2016). Substitution of clay content for P-remaining as an index of the phosphorus buffering capacity for soils of Rio Grande do Sul. *Revista Brasileira de Ciência do Solo*, *40*, 1-14. DOI: https://doi.org/10.1590/18069657rbcs20140535

Ruiz, H. A. (2005). Incremento da exatidão da análise granulométrica do solo por meio da coleta da suspensão (silte + argila). *Revista Brasileira de Ciência do Solo*, *29*(2), 297-300. DOI: https://doi.org/10.1590/S0100-06832005000200015

Santos, J. C., Le Pera, E., Oliveira, C. S., Souza Júnior, V. S., Pedron, F. A., & Corrêa, M. M. (2019). Impact of weathering on REE distribution in soil-saprolite profiles developed on orthogneisses in Borborema Province, NE Brazil. *Geoderma*, *347*, 103-117. DOI: https://doi.org/10.1016/j.geoderma.2019.03.040

Shah, T. I., Rai, A. P., & Azis, M., A. (2019). Relationship of phosphorus fractions with soil properties in mothbean growing acid soils of North Western Indian Himalayas. *Communications in Soil Science and Plant Analysis, 50*(9), 1192-1198. DOI: https://doi.org/10.1080/00103624.2019.1604730

Shariatmadari, H., Shirvani, M., & Dehghan, R. A. (2007). Availability of organic and inorganic phosphorus fractions to wheat in toposequences os calcareous soils. *Communications in Soil Science and Plant Analysis, 38*(19-20), 2601-2617. DOI: https://doi.org/10.1080/00103620701662810

Shiker, M. A. K. (2012). Multivariate statistical analysis. *British Journal of Science, 6*, 55-66.

Silva, F. A. S., & Azevedo, C. A. V. (2016). The ASSISTAT software version 7.7 and its use in the analysis of experimental data. *African Journal of Agricultural Research*, *11*(39), 3733-3740. DOI: https://doi.org/10.5897/AJAR2016.11522

Snedecor, G. W., & Cochran, W. G. (1967). *Statistical methods*. Iowa, US: Iowa State University Press.

Souza Júnior, R. F., Oliveira, F. H. T., Santos, H. C., Freire, F. J., & Arruda, J. A. (2012). Frações de fósforo inorgânico do solo e suas correlações com o fósforo quantificado por extratores e pelo milho. *Revista Brasileira de Ciência do Solo*, *36*(1), 159-169. DOI: https://doi.org/10.1590/S0100-06832012000100017

Tamfuh, P. A., Temgoua, E., Onana, V. L., Wotchoko, P., Tabi, F. O., & Bitom, D. (2018). Nature and genesis of Vertisols and North Cameroon management experience: A review. *Journal of Geosciences and Geomatics*, *6*(3), 124-137. DOI: https://doi.org/10.12691/jgg-6-3-3

Teixeira, P. C., Donagemma, G. K., Fontana, A., & Teixeira, W. G. (2017). *Manual de métodos de análise de solos*. Rio de Janeiro, RJ: Embrapa.

Tipping, E., Somerville, C. J., & Luster, J. (2016). The C:N:P:S stoichiometry of soil organic matter. *Biogeochemistry*, *130*, 117–131. DOI: https://doi.org/10.1007/s10533-016-0247-z

Wei, S., Tan, W., Liu, F., Zhao, W., & Weng, L. (2014). Surface properties and phosphate adsorption of binary systems containing goethite and kaolinite. *Geoderma*, *213*, 478–484. DOI: https://doi.org/10.1016/j.geoderma.2013.09.001

Yang, X., Chen X., & Yang, X. (2019). Effect of organic matter on phosphorus adsorption and desorption in a black soil from Northeast China. *Soil & Tillage Research, 187*, 85-91. DOI: https://doi.org/10.1016/j.still.2018.11.016

Zhang, T., Zhan, X., He, J., Feng, H., & Kang, Y. (2018). Salt characteristics and soluble cations redistribution in an impermeable calcareous saline-sodic soil reclaimed with an improved drip irrigation. *Agricultural Water Management*, *197*(C), 91-99. DOI: https://doi.org/10.1016/j.agwat.2017.11.020